

# AC-LIO: Towards Asymptotic and Consistent Convergence in LiDAR-Inertial Odometry

Tianxiang Zhang<sup>1</sup> Xuanxuan Zhang<sup>1</sup> Wenlei Fan<sup>1</sup> Xin Xia<sup>2</sup> You Li<sup>1</sup>

**Abstract**—Existing LiDAR-Inertial Odometry (LIO) frameworks typically utilize prior state trajectories derived from IMU integration to compensate for the motion distortion within LiDAR frames, and demonstrate outstanding accuracy and stability in regular low-speed and smooth scenes. However, in high-speed or intense motion scenarios, the residual distortion may increase due to the limitation of IMU’s accuracy and frequency, which will degrade the consistency between the LiDAR frame with its represented geometric environment, leading pointcloud registration to fall into local optima and consequently increasing the drift in long-time and large-scale localization.

To address the issue, we propose a novel asymptotically and consistently converging LIO framework called AC-LIO. First, during the iterative state estimation, we backwards propagate the update term based on the prior state chain, and asymptotically compensate the residual distortion before next iteration. Second, considering the weak correlation between the initial error and motion distortion of current frame, we propose a convergence criteria based on pointcloud constraints to control the back propagation. The approach of guiding the asymptotic distortion compensation based on convergence criteria can promote the consistent convergence of pointcloud registration and increase the accuracy and robustness of LIO. Experiments show that our AC-LIO framework, compared to other state-of-the-art frameworks, effectively promotes consistent convergence in state estimation and further improves the accuracy of long-time and large-scale localization and mapping.

## I. INTRODUCTION

With the development of Simultaneous Localization and Mapping (SLAM) technology, the perception of robots on the external environment and their own motion is becoming more and more precise [1, 2]. As a key branch, LiDAR-Inertial Odometry (LIO) has gained widespread application in autonomous driving, unmanned logistics and other fields, for its high robustness and accuracy [3, 4]. Compared to Visual-Inertial Odometry (VIO), the LIO system can directly obtain depth observations of surroundings [5], without the need to estimate the depth of feature points [6, 7], and exhibits better adaptability to different lighting conditions [8, 9].

This work was supported in part by the National Key R&D Program of China (2023YFB3906600, 2022YFE0139300, 2022YFB3903800), the Major Science and Technologu Projects in Hubei Province (2022AAA009), and the National Natural Science Foundation of China (42274052).

<sup>1</sup>Tianxiang Zhang, Xuanxuan Zhang, Wenlei Fan, and You Li are with State Key Laboratory of Information Engineering in Surveying, Mapping and Remote Sensing (LIESMARS), Wuhan University, 430072, China. Xuanxuan Zhang is the corresponding author. Email: {cyberkona; xuanxuanzhang; wenleifan; liyou}@whu.edu.cn

<sup>2</sup>Xin Xia is with Department of Civil and Environmental Engineering, UCLA Samueli School of Engineering, Los Angeles, CA 90095. Email: x35xia@ucla.edu

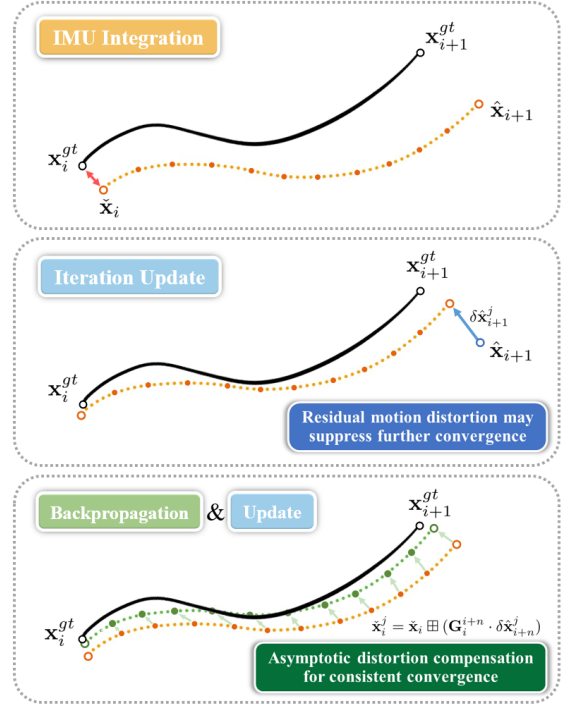


Fig. 1. The basic principle of AC-LIO framework. Conventional LIO typically consider initial distortion compensation via IMU integration, yet the residual distortion may prevent the registration from further convergence. In contrast, our AC-LIO employs an asymptotic backpropagation strategy to promote consistent convergence in state estimation.

However, as LIO system continues to evolve, there still remain several fundamental issues to be addressed [10, 11], one of which is the conflict between continuous motion and rigid pointcloud registration [12]. Since the acquisition of LiDAR stream is often accompanied with the ego-motion of vehicle, the laser points with different timestamps actually lie in different coordinate frames.

Existing frameworks typically only consider using IMU integration for the initial compensation of motion distortion [13]–[15], without further optimization of the residual distortion in state estimation. But in high-speed or violent motion scenarios, the residual motion distortion tends to increase due to the limitations of IMU’s accuracy and frequency, which would suppress further convergence of pointcloud registration and decrease odometry accuracy in long-term, large-scale scenarios [16].

To address this, we propose AC-LIO, a novel asymptotically and consistently converging LIO framework. First, during the iterative state estimation, we backwards propagate the current update term based on the prior state chain,

and asymptotically compensate the residual distortion before next iteration. This approach could enhance the consistency between the current LiDAR frame and the represented geometric environment, and avoid the pointcloud registration from falling into local optimum due to the residual distortion, thereby promoting the consistent convergence of state estimation and improving the accuracy of long-time and large-scene localization. Compared to other strategies such as continuous-time estimation or frame segmentation, our method can be seamlessly embedded into the iterative Kalman Filter framework [17], offering great flexibility and scalability.

Second, considering the weak correlation between the initial error and motion distortion of current frame, we also propose a convergence criteria based on the point-plane residuals to control the back propagation. This strategy ensures, We use this criteria to evaluate the convergence of the pointcloud registration, ensuring the backpropagation and asymptotic compensation only happens under the condition of sufficient convergence in previous LiDAR frame, and thus guaranteeing the robustness of LIO system.

In summary, our main contributions are as follows:

- We implement a novel asymptotically and consistently converging LIO framework. During the iterative update, we back propagate the current update term based on the prior state chain, and asymptotically compensate the residual distortion before next iteration, promoting the consistent convergence of registration and improving the accuracy in long-time and large-scale scenarios.
- We introduce a convergence criteria based on point-plane residuals to control the back propagation. We utilize the criteria to evaluate the convergence of registration, ensuring the back propagation to be performed only upon sufficient convergence of the previous registration, thus further enhancing the system robustness.
- Our method can be easily and seamlessly integrated into traditional iterative Kalman Filter framework. Compared to other optimization strategies for motion distortion, our framework introduce no extra estimates or states, making the asymptotic compensation less computationally expensive but highly flexible and scalable.
- We conduct extensive experiments on AC-LIO in a series of real-world datasets with various scenarios. The results show that our proposed AC-LIO exhibits higher accuracy in long-term localization compared to the state-of-the-art open-source methods.

## II. RELATED WORK

Since the motion distortion can degrade the consistency between the pointcloud and the geometric environment, and thus suppress the sufficient convergence of registration. To mitigate the adverse effect of motion distortion, existing LiDAR(-inertial) odometry adopt various strategies to appropriately compensate for this distortion.

For LiDAR-only odometry, most studies utilize the constant velocity model to compensate for motion aberrations. Studies such as LOAM [18] and Lego-LOAM [19] have

achieved significant effects with the assumption of constant velocity motion during the corresponding time of LiDAR frames. However, this assumption only works effectively when LiDAR frame interval is enough short and the motion is slow and smooth. In case of drastic velocity variation, the constant velocity model cannot accurately characterize the current motion state, and this will result in increased drift and even odometry divergence.

As for LiDAR-inertial odometry, the IMU observation can provide relatively reliable prior state information. This provides a new scheme for compensating motion distortion via IMU integration. FAST-LIO [20] employs the IMU state backpropagation to correct the distorted pointcloud, and then conducts state estimation through Error State Kalman Filter. LIO-SAM [21] utilizes the IMU pre-integration to de-skew pointcloud, and combines multiple constraints including LiDAR, IMU, and GPS through the factor graph. Although these methods can mitigate the impact of pointcloud distortion to some extent, there are still some limitations without considering the further optimization of residual motion distortion.

To characterize trajectory more precisely in state estimation, many frameworks come up with new optimization solutions. As pure LiDAR framework, I<sup>2</sup>EKF-LO [22] utilizes additional iteration to specifically estimate motion distortion, this approach can suppress distortion but the extra iteration may sacrifice computational efficiency. CLINS [23] introduces the B-spline model [24] for continuous time state estimation. However, the unconstrained trajectory would not always conform to the B-spline model due to time resolution limitations in high-speed, dynamic motion. Moreover, the continuous-time optimization strategy may introduce a higher computational cost. Point-LIO [25] adopts a point-by-point update strategy to avoid the motion distortion issue and realize extremely high-frequency odometry. Compared to frame based registration, the point-by-point strategy is more likely to degenerate in adverse scenarios. FR-LIO [26] divides the LiDAR frame into several sub-frames based on IMU observation. This approach can increase the system update frequency, thus reducing the impact of motion distortion. Besides, FR-LIO strengthens the constraints between subframes via RTS smoother [27], but still faces the risk of subframe degradation.

In contrast, our proposed AC-LIO framework utilizes the convergence criteria to guide the backpropagation process, to achieve the asymptotic compensation of residual motion distortion. As a result, our approach can promote the consistent convergence of pointcloud registration during iterative update, further improving the accuracy over long-term and large-scale scenarios while ensuring the system robustness.

## III. METHODOLOGY

### A. System Overview

The system overview of our AC-LIO framework is shown in Fig. 2. IMU observations are fed into the forward propagation module for integration to obtain prior trajectories. Then, the LiDAR data utilize the prior state chain for initial

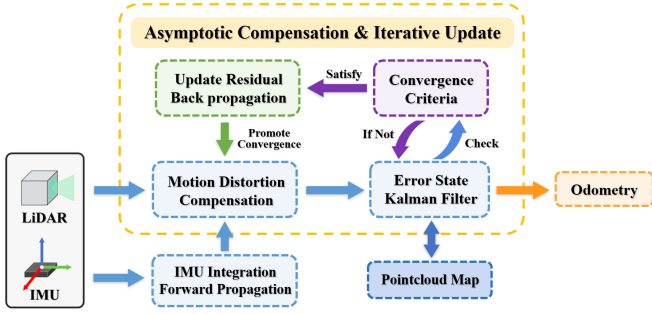


Fig. 2. The system overview of our AC-LIO framework. During iterative ESKF, asymptotic compensation of pointcloud distortion will be conducted based on the convergence criteria, to promote consistent convergence of state estimation.

compensation, next passed into the Error State Kalman Filter (ESKF) for state estimation [28], where the average point-to-plane residual (APR) is calculated after each update.

During the iteration, if the APR of previous LiDAR frame is lower than the convergence criteria and the current APR exceeds it, then the backpropagation of update residual will be executed. After backpropagation, the LiDAR frame needs to be re-compensated to promote the consistent convergence of state estimation. Otherwise, if the conditions are not met, the backpropagation will be skipped and iteration continues. Once reaching the maximum of iterations, the system will merge the LiDAR frame under the posterior pose into pointcloud map and publish the current odometry.

### B. ESKF State Estimation

For efficiency and accuracy concerns, the AC-LIO we proposed utilizes the ESKF framework for state estimation. Based on the kinematic model and IMU measurement model, the state  $\mathbf{x}$ , input  $\mathbf{i}$ , and noise  $\mathbf{n}$  can be defined as follows:

$$\begin{aligned} \mathbf{x} &\doteq [\mathbf{R}_I^G \quad \mathbf{p}_I^G \quad \mathbf{v}_I \quad \mathbf{b}_\omega \quad \mathbf{b}_a \quad \mathbf{g}^G]^T \\ \mathbf{i} &\doteq [\boldsymbol{\omega}_m \quad \mathbf{a}_m]^T \\ \mathbf{n} &\doteq [\mathbf{n}_\omega \quad \mathbf{n}_a \quad \mathbf{n}_{b\omega} \quad \mathbf{n}_{ba}]^T \end{aligned} \quad (1)$$

Where  $G$  and  $I$  denote the global and the IMU frames,  $\mathbf{R}_I^G$ ,  $\mathbf{p}_I^G$  and  $\mathbf{v}_I^G$  are IMU's orientation, position and linear velocity in  $G$ , and  $\mathbf{g}^G$  is the local gravity. The  $\mathbf{n}_\omega$ ,  $\mathbf{n}_a$  are noises of angular velocity  $\boldsymbol{\omega}_m$  and linear acceleration  $\mathbf{a}_m$ , the  $\mathbf{b}_\omega$ ,  $\mathbf{b}_a$  are IMU bias with  $\mathbf{n}_{b\omega}$  and  $\mathbf{n}_{ba}$  as their noises in Gaussian-Markov model.

Since  $\mathbf{x}$  can be regarded as a high-dimensional manifold locally homeomorphic to Euclidean space  $\mathbb{R}$ . The operations  $\boxplus$  and  $\boxminus$  on manifold can be defined according to [29]. Note the error state as  $\delta\mathbf{x}$ , the recursion for  $\delta\mathbf{x}$  and covariance  $\mathbf{P}$  can be expressed as follows:

$$\begin{aligned} \delta\mathbf{x}_i &\doteq [\delta\boldsymbol{\theta} \quad \delta\mathbf{p}_I^G \quad \delta\mathbf{v}_I \quad \delta\mathbf{b}_\omega \quad \delta\mathbf{b}_a \quad \delta\mathbf{g}^G]^T \\ \delta\hat{\mathbf{x}}_{i+1} &= \mathbf{F}_a\delta\hat{\mathbf{x}}_i + \mathbf{F}_n\mathbf{n}_i \\ \hat{\mathbf{P}}_{i+1} &= \mathbf{F}_a\hat{\mathbf{P}}_i\mathbf{F}_a^T + \mathbf{F}_n\mathbf{Q}\mathbf{F}_n^T \end{aligned} \quad (2)$$

Denote  $\mathbf{T}_L^I$  is the extrinsic between LiDAR and IMU, then the pointcloud can be transformed to frame  $I$  via the prior pose chain. For a point  $\mathbf{p}$  in LiDAR frame, its neighboring

cluster can be searched by KNN in pointcloud map. A plane is then fitted to this cluster and we obtain the normal vector  $\mathbf{u}$ . Note one point of the cluster as  $\mathbf{q}$  and  $(\cdot)_\wedge$  as the upper triangular matrix of vector, then the point-plane residual  $\mathbf{z}$  and measurement matrix  $\mathbf{H}$  are as follows:

$$\begin{aligned} \mathbf{z} &= \mathbf{u}(\hat{\mathbf{p}}^G - \mathbf{q}^G)^T \\ \mathbf{H} &= [-\mathbf{u}\hat{\mathbf{R}}_I^G(\mathbf{T}_L^I\mathbf{p}^L)_\wedge \quad \mathbf{u} \quad \mathbf{0}_{3\times 12}] \end{aligned} \quad (3)$$

Considering the nonlinear errors in the  $\mathbf{F}_a$ ,  $\mathbf{F}_n$  and  $\mathbf{H}$ , the estimation may require iteration to promote convergence. Let  $\mathbf{A}$  denote the Jacobian of update component with respect to  $\delta\mathbf{x}$ , and according to [13], the update equation is:

$$\begin{aligned} \mathbf{K} &= \mathbf{P}\mathbf{H}^T(\mathbf{H}\mathbf{P}\mathbf{H}^T + \mathbf{R})^{-1} \\ \hat{\mathbf{x}}_{i+1}^{j+1} &= \hat{\mathbf{x}}_{i+1}^j \boxplus [-\mathbf{K}\mathbf{z} - (\mathbf{I} - \mathbf{K}\mathbf{H})(\mathbf{A}^j)^{-1}(\hat{\mathbf{x}}_{i+1}^j \boxminus \hat{\mathbf{x}}_{i+1})] \end{aligned} \quad (4)$$

Once the update term is less than a preset threshold, the solution can be considered to converge.

$$\check{\mathbf{x}}_{i+1} \leftarrow \hat{\mathbf{x}}_{i+1}^{j+1}, \check{\mathbf{P}}_{i+1} \leftarrow (\mathbf{I} - \mathbf{K}\mathbf{H})\hat{\mathbf{P}}_{i+1} \quad (5)$$

With the iterative update of ESKF, our AC-LIO could further promote the consistent convergence of the state estimation via the asymptotic distortion compensation and convergence criteria introduced in following sections.

### C. Asymptotic Distortion Compensation

In smooth motion scenarios, an initial compensation of motion distortion via IMU integration can basically satisfy the accuracy demand. However, when encountering violent motion scenarios, the residual motion distortion may increase due to the limitation of IMU's frequency and accuracy. Compared to the noise of LiDAR observations, motion distortion may introduce bias in pointcloud registration, making it difficult to utilize the statistical properties of pointcloud to mitigate the adverse effects on state estimation.

With reference to the fixed interval smooth strategy, we selectively back propagate the update term  $\delta\mathbf{x}$  based on the prior state chain during iteration. The noise between adjacent states can be expressed as follows:

$$\begin{aligned} \delta\check{\mathbf{x}}_i &\sim \mathcal{N}(\mathbf{0}_{18\times 1}, \check{\mathbf{P}}_i) \\ \delta\check{\mathbf{x}}_{i+1} &\sim \mathcal{N}(\mathbf{0}_{18\times 1}, \mathbf{F}_a\check{\mathbf{P}}_i\mathbf{F}_a^T + \mathbf{F}_n\mathbf{Q}\mathbf{F}_n^T) \end{aligned} \quad (6)$$

During the on-manifold propagation of state  $\mathbf{x}$ , the noise of current error state  $\delta\check{\mathbf{x}}_{i+1}$  consists of the propagation of previous state  $\delta\check{\mathbf{x}}_i$  and the accumulated process noise. According to RTS smooth strategy [27], the contribution of previous state in current update term just corresponds to the proportion of the propagation covariance  $\mathbf{F}_a\check{\mathbf{P}}_i\mathbf{F}_a^T$  within current covariance  $\check{\mathbf{P}}_{i+1}$ . Consequently, the gain matrix  $\mathbf{G}$  and the backward recursion of  $\delta\mathbf{x}$  can be denoted as follows:

$$\begin{aligned} \mathbf{G} &= \check{\mathbf{P}}_i\mathbf{F}_a^T\hat{\mathbf{P}}_{i+1}^{-1} \\ \delta\check{\mathbf{x}}_i^j &= \mathbf{G} \cdot \delta\check{\mathbf{x}}_{i+1}^j \end{aligned} \quad (7)$$

Furthermore, since there may exist numerous IMU states to maintain within the timeperiod of LiDAR frame, a sequential backward recursion can characterize the smoothed trajectory precisely. However, from an overall perspective, this

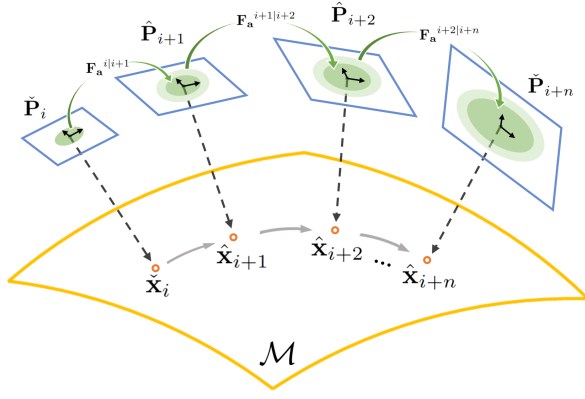


Fig. 3. The on-manifold propagation. The noise of current state involves the process noise and the propagation of previous state, the update term can be recursive backward according to this relationship.

treatment will increase much computational cost in iterative ESKF, but cannot bring additional accuracy improvement in subsequent asymptotic distortion compensation. Compared to state-by-state backpropagation, selectively updating several anchors in the prior state chain can further reduce the computational cost with little accuracy loss. To this end, we extend the backwards recursion to any states within the LiDAR frame, thereby reducing the computational complexity of backpropagation and distortion compensation.

$$\begin{aligned} \mathbf{F}_a^{i|i+n} &= \prod_{k=i}^{i+n-1} \mathbf{F}_a^{k|k+1} \\ \mathbf{G}_i^{i+n} &= \tilde{\mathbf{P}}_i (\mathbf{F}_a^{i|i+n})^T (\tilde{\mathbf{P}}_{i+n})^{-1} \\ \tilde{\mathbf{x}}_i^j &= \tilde{\mathbf{x}}_i \boxplus (\mathbf{G}_i^{i+n} \cdot \delta \tilde{\mathbf{x}}_{i+n}^j) \end{aligned} \quad (8)$$

After each backpropagation of the update term  $\tilde{\mathbf{x}}_{i+n}^j$ , the residual pointcloud distortion can continue to be compensated based on the smoothed trajectory. For the point  $\mathbf{p}^L$  in LiDAR frame, and the state corresponding to its timestamp  $t$  after the  $j$ th backpropagation can be denoted as  $\tilde{\mathbf{x}}_t^j$ , then the updated coordinates can be noted as:

$$\hat{\mathbf{p}}_j^G = \mathbf{T}(\tilde{\mathbf{x}}_t^j) \mathbf{T}_L^T \mathbf{p}^L \quad (9)$$

Where  $\mathbf{T}(\mathbf{x})$  represents the transformation matrix of state  $\mathbf{x}$  in frame  $G$ . As the iterative ESKF converges, the final solution of the backward propagation can be expressed as:

$$\bar{\mathbf{x}}_i \leftarrow \tilde{\mathbf{x}}_i^{j+1}, \bar{\mathbf{P}}_i \leftarrow \mathbf{G}_i^{i+n} \tilde{\mathbf{P}}_{i+n} (\mathbf{G}_i^{i+n})^T \quad (10)$$

In practice, if there is no need to reuse the previous state queue in next frame, the covariance update after backpropagation can be skipped for efficiency.

#### D. Convergence Criteria

In order to exploit the statistical properties of the pointcloud, during the iterative state estimation, we select the mean value of the point-to-plane residual (abbreviated as APR above), as the criteria for evaluating the convergence of pointcloud registration. For simplification, assuming the pointcloud registration fully converges to the global optimum, considering the ranging accuracy of LiDAR and

the construction of point-to-plane residual, we can roughly model the expectation of the APR, to provide a threshold reference for the convergence criteria.

Denote the fitted plane in pointcloud map as  $S$  with its normal vector as  $\mathbf{u}$ , and the point-plane residual as  $\mathbf{z}$ . Then, the incident angle  $\phi$  of point  $\mathbf{p}$  with respect to plane  $S$  can be expressed as:

$$\phi = \arccos \frac{|\mathbf{u} \cdot \mathbf{p}|}{|\mathbf{u}| \cdot |\mathbf{p}|} \quad (11)$$

When the laser beam is perpendicular to plane  $S$ , then the incident angle  $\phi$  will be zero. Assuming that the ranging error  $\mathbf{n}_p$  of laser point follows Gaussian distribution with zero mean and  $\sigma$  variance, then the residual  $\mathbf{z}_\perp$  will follow chi-squared distribution and can be expressed as follows:

$$\begin{aligned} \mathbf{p}^L &= \mathbf{p}_{gt}^L + \mathbf{n}_p, \mathbf{n}_p \sim \mathcal{N}(0, \sigma) \\ \mathbf{z}_\perp &= |\mathbf{p}_{gt}^L - \mathbf{p}^L| \\ \frac{\mathbf{z}_\perp^2}{\sigma^2} &\sim \chi^2(1), \mathbb{E}(\mathbf{z}_\perp) = \sigma \end{aligned} \quad (12)$$

As the surrounding environment varies during ego-motion, the distribution of normal vector  $\mathbf{n}$  of plane  $S$  will also change. Eventually, the variation of the geometrical scene will be reflected in the distribution of the incident angle  $\phi$ . Assuming the incident angle is uniformly distributed over the domain  $[0, \pi/2]$ , then the expected mean of the point-plane residual  $\mathbf{z}$  can be expressed as:

$$\mathbb{E}(\mathbf{z}) = \frac{2}{\pi} \int_0^{\frac{\pi}{2}} \mathbb{E}(\mathbf{z}_\perp) \cos \phi \, d\phi = \frac{2}{\pi} \sigma \quad (13)$$

Therefore, assuming the pointcloud registration converges to the global optimum, and only considering the LiDAR ranging error, the expectation of APR should be  $2\sigma/\pi$ . If the mean value of current point-plane residual is lower than this criteria, then the last registration can be considered as sufficiently converged.

According to the threshold of convergence criteria, we can easily determine the convergence degree of pointcloud registration, and control the backpropagation and the asymptotic distortion compensation. Noting that  $\sigma_t = \mathbb{E}(\mathbf{z})$  and the selected threshold of convergence criteria as  $\eta$ , due to the factors such as dynamic objects and cumulative errors in pointcloud map, the threshold  $\eta$  can be appropriately extended to the interval of  $[\sigma_t, 2\sigma_t]$  in practice.

In particular, we perform two conditional judgments in iterative state estimation: First, evaluate the previous LiDAR frame, if the APR is less than the threshold, it is considered to be sufficiently converged and we can continue. Then, check the convergence of current registration, if the APR is still less than the threshold, there is no need to backpropagate for small residual distortion; otherwise, perform the backpropagation and asymptotic compensation, in order to promote the consistent convergence in state estimation.

The approach, on one hand, can ensure the backpropagation and asymptotic compensation only performed as the previous LiDAR frame converged well, thus enhancing the odometry robustness in long-time, large-scale scenario;



Fig. 4. Our handheld sensor suite used in self-collected dataset, including the solid-state LiDAR Livox Avia with the built-in BMI088 IMU, and three other cameras.

on the other hand, can avoid lots of additional operations in unreliable or unnecessary conditions, further saving the system computational expense. The experiment results of our framework are shown in the next section.

#### IV. EXPERIMENT RESULTS

In this section, we qualitatively and quantitatively evaluate AC-LIO framework through a series of experiments with various public and self-collected datasets. To examine the accuracy improvement of our approach in long-time and large-scale scenarios, and the effect of convergence criteria on system robustness, we conduct extensive experiments on the odometry accuracy and the validity of convergence criteria.

##### A. Odometry Accuracy Evaluation

In the odometry accuracy experiments, we compare AC-LIO framework with current state-of-the-art LIO systems including FAST-LIO2 and Point-LIO. All algorithms are implemented in C++ and employed on an i9 CPU desktop computer with the ROS operating system in Ubuntu. These methods only utilize CPU for computation without the assistance of GPU parallel computing. Besides, in the odometry accuracy experiments, we maintain the threshold of convergence criteria in the extended interval, i.e.,  $\eta \in [\sigma_t, 2\sigma_t]$ . A brief introduction of the public and self-collected handheld datasets is provided below:

- WHU-Helmet [30]: Collected on compact helmet system, the dataset contains complex large-scale scenes including wild, urban and tunnel, with challenges of drastic motion from wearer and repeated symmetrical geometric structures. The datasets used include *Residence\_5.2*, *Park\_3.2*, *Subway\_3.3*, *Mall\_6.3*.
- BotanicGarden [31]: Mounted on all-terrain wheeled robot, this dataset consists of diverse natural scenes including riversides, narrow trails and bridges. The datasets used include the *Garden* series.
- Handheld datasets: We collected multiple datasets of different scenarios and motion conditions, covering indoor and outdoor scenes like library, campus road and

TABLE I  
ODOMETRY ACCURACY EVALUATION - RMSE OF ATE ( $m$ )

	AC-LIO(Ours)	FAST-LIO2	Point-LIO
<i>Residence_5.2</i> (452.9m)	<b>0.415</b>	0.505	– <sup>1</sup>
<i>Park_3.2</i> (628.9m)	<b>0.582</b>	0.618	–
<i>Subway_3.3</i> (827.0m)	<b>1.670</b>	3.752	–
<i>Mall_6.3</i> (1006.5m)	0.216	<b>0.208</b>	15.409
<i>Garden_1005</i> (566.8m)	<b>0.773</b>	1.053	0.917
<i>Garden_1006</i> (686.2m)	<b>1.796</b>	2.075	2.471
<i>Garden_1008</i> (855.9m)	<b>1.152</b>	1.577	1.590

<sup>1</sup> – means that the system severely diverged midway.

TABLE II  
ODOMETRY ACCURACY EVALUATION - END TO END ERRORS ( $m$ )

	AC-LIO(Ours)	FAST-LIO2	Point-LIO
<i>Indoor_1</i> (~100m)	<b>0.8929</b>	1.1330	5.4006
<i>Indoor_2</i> (~100m)	0.2267	0.2043	<b>0.1636</b>
<i>Indoor_3</i> (~100m)	<b>1.5959</b>	3.0011	6.8438
<i>Outdoor_1</i> (~300m)	<b>0.1378</b>	1.9007	0.7280
<i>Outdoor_2</i> (~400m)	<b>0.9840</b>	2.1944	1.2607
<i>Outdoor_3</i> (~500m)	<b>2.6659</b>	4.7023	4.6066

UAV airfield. The handheld data collection device is shown in Fig. 4. The datasets used include *Indoor* and *Outdoor* series.

In the evaluation of WHU-Helmet, Point-LIO diverged midway in the *Residence\_5.2* and *Subway\_3.3* due to severe motion combined with locally degraded scenarios, and diverged in *Park\_3.2* due to extensive occlusion by pedestrians. And in *Mall\_6.3*, the system experienced significant drift during turns due to the reflection from glass walls of the shopping mall. In the first three datasets, our AC-LIO framework effectively resists the challenging scenarios mentioned above and outperformed the FAST-LIO in long-term, large-scale localization accuracy. Only in the last dataset of WHU-Helmet slightly lower than FAST-LIO.

For the BotanicGarden datasets, since the sensors are mounted on a wheeled robotic platform, the overall motion is smooth and suitable for evaluating the long-duration drift under regular motion conditions. Across the three LIO-robags provided by BotanicGarden, the AC-LIO demonstrates higher accuracy, exhibiting better convergence in long-term localization.

Next is the evaluation of handheld datasets. In *Indoor\_1* UAV airfield and *Indoor\_3* library scenarios, we conduct intense turning in narrow environment. And in the *Indoor\_2* garage scene, with smooth motion and highly structured sur-

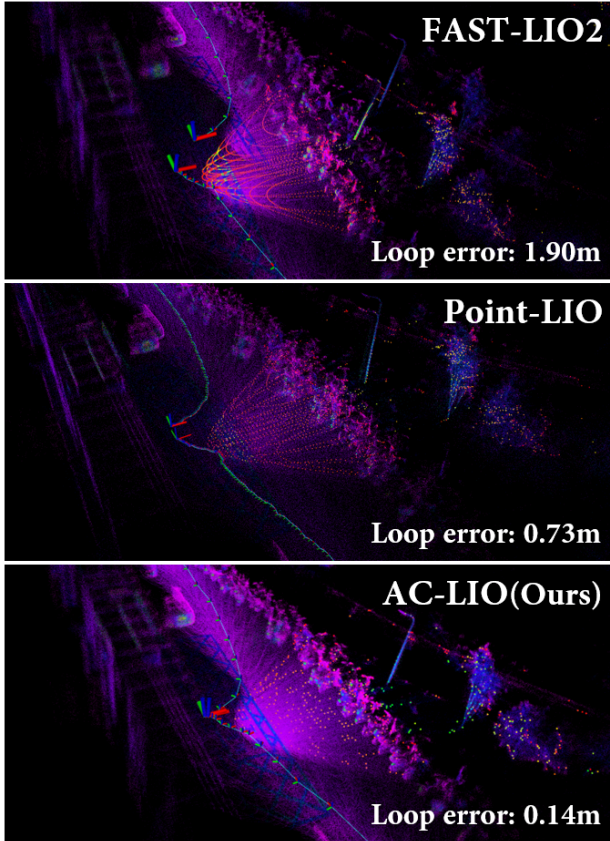


Fig. 5. Accuracy evaluation in campus road scene. The figure shows the result of *Outdoor.1*. We keep running after initialization to enhance the motion intensity and complete a closed loop about 300m. The closure trajectory and the map consistency suggest that our AC-LIO achieves better performance.

roundings, Point-LIO achieves higher closed-loop accuracy. Then in the *Outdoor* sequences, we handhold the device and attempt different motion conditions including running and sharp turns in campus road scenes.

Concrete experiment results are demonstrated in Table I, Table II and Fig. 5. The results indicate the AC-LIO framework generally outperforms the FAST-LIO2 and Point-LIO in terms of accuracy during long-term, large-scale scenes, and exhibits high robustness under challenging scenarios.

### B. Convergence Criteria Validity Evaluation

To evaluate the validity of the proposed convergence criteria, we examine the odometry accuracy at different  $\eta$  threshold levels. While keeping other parameters the same, we only adjust the threshold of convergence criteria. Due to the factors such as dynamic objects, cumulative pointcloud map errors, etc., we fine-tune the threshold  $\eta$  within the interval of  $[\sigma_t, 2\sigma_t]$ . The specific experimental results are shown in Table III.

- $\eta = 0$ : No backpropagation and asymptotic compensation is performed at this situation, reflecting the basic accuracy of the odometry.
- $\eta = 0.5\sigma_t$ : Lower than the expected mean of pointcloud residuals, rarely perform backpropagation. (Only considering LiDAR ranging errors,  $\mathbb{E}(\mathbf{z}) = \sigma_t$ )

TABLE III

CONVERGENCE CRITERIA VALIDITY EVALUATION - RMSE OF ATE ( $m$ )

	0	$0.5\sigma_t$	$[\sigma_t, 2\sigma_t]$	$3\sigma_t$
<i>Park_3.2</i> (628.9m)	0.624	0.610	<b>0.582</b>	0.616
<i>Subway_3.3</i> (827.0m)	2.841	2.419	<b>1.670</b>	1.788
<i>Garden_1006</i> (686.2m)	1.901	<b>1.709</b>	1.796	1.892
<i>Garden_1008</i> (855.9m)	1.197	1.199	<b>1.152</b>	1.178

- $\eta \in [\sigma_t, 2\sigma_t]$ : Recommended interval in consideration of other error factors, assuring the backpropagation and asymptotic compensation will be performed with sufficient convergence in previous frame.
- $\eta = 3\sigma_t$ : Too high a threshold may lead to backpropagation in case of large initial errors, potentially damaging the system's accuracy and robustness.

The experimental results show that, in most cases, selecting the threshold  $\eta$  within the range of  $[\sigma_t, 2\sigma_t]$  achieved higher accuracy. Overall, as the threshold increases from zero, the odometry accuracy initially improves because more sufficiently converged states are allowed to perform backpropagation and asymptotic compensation. However, as the threshold increases further, states with larger initial errors are also allowed to backpropagate, which reduces the effectiveness of the asymptotic compensation and negatively impacts odometry accuracy.

## V. CONCLUSIONS

In this paper, we propose AC-LIO, a novel asymptotically and consistently converging LIO framework. We reconsider the factors that may introduce errors in long-duration, large-scale scenarios, aiming to further enhance the convergence of the odometry. First, during iterative state estimation, we backpropagate the update term along the prior state chain and asymptotically compensate for residual distortion before the next iteration. Second, considering the weak correlation between the initial error and motion distortion in the current frame, we propose a convergence criteria based on pointcloud constraints to control backpropagation. In summary, the approach of guiding asymptotic compensation based on convergence criteria is designed to promote the consistent convergence of pointcloud registration, ensuring robustness while further improving the odometry accuracy.

We conducted a series of experiments on public and self-collected datasets, covering various scenarios and motion conditions across multiple scales. The experiments show that, compared to other state-of-the-art frameworks, our AC-LIO framework effectively promotes consistent convergence in state estimation and further enhances the accuracy of long-term, large-scale localization and mapping.

## REFERENCES

- [1] H. Taheri and Z. C. Xia, "Slam: definition and evolution," *Engineering Applications of Artificial Intelligence*, vol. 97, p. 104032, 2021.

- [2] C. Cadena, L. Carlone, H. Carrillo, Y. Latif, D. Scaramuzza, J. Neira, I. Reid, and J. J. Leonard, "Past, present, and future of simultaneous localization and mapping: Toward the robust-perception age," *IEEE Transactions on robotics*, vol. 32, no. 6, pp. 1309–1332, 2016.
- [3] Y. Li and J. Ibanez-Guzman, "Lidar for autonomous driving: The principles, challenges, and trends for automotive lidar and perception systems," *IEEE Signal Processing Magazine*, vol. 37, no. 4, pp. 50–61, 2020.
- [4] R. Roriz, J. Cabral, and T. Gomes, "Automotive lidar technology: A survey," *IEEE Transactions on Intelligent Transportation Systems*, vol. 23, no. 7, pp. 6282–6297, 2021.
- [5] M. U. Khan, S. A. A. Zaidi, A. Ishtiaq, S. U. R. Bukhari, S. Samer, and A. Farman, "A comparative survey of lidar-slam and lidar based sensor technologies," in *2021 Mohammad Ali Jinnah University International Conference on Computing (MAJICC)*. IEEE, 2021, pp. 1–8.
- [6] G. Huang, "Visual-inertial navigation: A concise review," in *2019 international conference on robotics and automation (ICRA)*. IEEE, 2019, pp. 9572–9582.
- [7] M. Servières, V. Renaudin, A. Dupuis, and N. Antigny, "Visual and visual-inertial slam: State of the art, classification, and experimental benchmarking," *Journal of Sensors*, vol. 2021, no. 1, p. 2054828, 2021.
- [8] T. Raj, F. Hanim Hashim, A. Baseri Huddin, M. F. Ibrahim, and A. Hussain, "A survey on lidar scanning mechanisms," *Electronics*, vol. 9, no. 5, p. 741, 2020.
- [9] D. Sharafutdinov, M. Griguletskii, P. Kopanov, M. Kurenkov, G. Ferrer, A. Burkov, A. Gonnochenko, and D. Tsetserukou, "Comparison of modern open-source visual slam approaches," *Journal of Intelligent & Robotic Systems*, vol. 107, no. 3, p. 43, 2023.
- [10] D. Lee, M. Jung, W. Yang, and A. Kim, "Lidar odometry survey: recent advancements and remaining challenges," *Intelligent Service Robotics*, pp. 1–24, 2024.
- [11] K. Li, M. Li, and U. D. Hanebeck, "Towards high-performance solid-state-lidar-inertial odometry and mapping," *IEEE Robotics and Automation Letters*, vol. 6, no. 3, pp. 5167–5174, 2021.
- [12] K. Chen, R. Nemiroff, and B. T. Lopez, "Direct lidar-inertial odometry: Lightweight lio with continuous-time motion correction," in *2023 IEEE international conference on robotics and automation (ICRA)*. IEEE, 2023, pp. 3983–3989.
- [13] W. Xu and F. Zhang, "Fast-lio: A fast, robust lidar-inertial odometry package by tightly-coupled iterated kalman filter," *IEEE Robotics and Automation Letters*, vol. 6, no. 2, pp. 3317–3324, 2021.
- [14] P. Pfreundschuh, H. Oleynikova, C. Cadena, R. Siegwart, and O. Andersson, "Coin-lio: Complementary intensity-augmented lidar inertial odometry," in *2024 IEEE International Conference on Robotics and Automation (ICRA)*. IEEE, 2024, pp. 1730–1737.
- [15] K. Huang, J. Zhao, J. Lin, Z. Zhu, S. Song, C. Ye, and T. Feng, "Log-lio2: A lidar-inertial odometry with efficient uncertainty analysis," *arXiv preprint arXiv:2405.01316*, 2024.
- [16] H. Yin, X. Xu, S. Lu, X. Chen, R. Xiong, S. Shen, C. Stachniss, and Y. Wang, "A survey on global lidar localization: Challenges, advances and open problems," *International Journal of Computer Vision*, pp. 1–33, 2024.
- [17] D. Simon, "Kalman filtering," *Embedded systems programming*, vol. 14, no. 6, pp. 72–79, 2001.
- [18] J. Zhang and S. Singh, "Loam: Lidar odometry and mapping in real-time." in *Robotics: Science and systems*, vol. 2, no. 9. Berkeley, CA, 2014, pp. 1–9.
- [19] T. Shan and B. Englot, "Lego-loam: Lightweight and ground-optimized lidar odometry and mapping on variable terrain," in *2018 IEEE/RSJ International Conference on Intelligent Robots and Systems (IROS)*. IEEE, 2018, pp. 4758–4765.
- [20] W. Xu, Y. Cai, D. He, J. Lin, and F. Zhang, "Fast-lio2: Fast direct lidar-inertial odometry," *IEEE Transactions on Robotics*, vol. 38, no. 4, pp. 2053–2073, 2022.
- [21] T. Shan, B. Englot, D. Meyers, W. Wang, C. Ratti, and D. Rus, "Lio-sam: Tightly-coupled lidar inertial odometry via smoothing and mapping," in *2020 IEEE/RSJ international conference on intelligent robots and systems (IROS)*. IEEE, 2020, pp. 5135–5142.
- [22] W. Yu, J. Xu, C. Zhao, L. Zhao, T.-M. Nguyen, S. Yuan, M. Bai, and L. Xie, "I2ekf-lo: A dual-iteration extended kalman filter based lidar odometry," *arXiv preprint arXiv:2407.02190*, 2024.
- [23] J. Lv, K. Hu, J. Xu, Y. Liu, X. Ma, and X. Zuo, "Clins: Continuous-time trajectory estimation for lidar-inertial system," in *2021 IEEE/RSJ International Conference on Intelligent Robots and Systems (IROS)*. IEEE, 2021, pp. 6657–6663.
- [24] M. Unser, A. Aldroubi, and M. Eden, "B-spline signal processing. i. theory," *IEEE transactions on signal processing*, vol. 41, no. 2, pp. 821–833, 1993.
- [25] D. He, W. Xu, N. Chen, F. Kong, C. Yuan, and F. Zhang, "Point-lio: Robust high-bandwidth light detection and ranging inertial odometry," *Advanced Intelligent Systems*, vol. 5, no. 7, p. 2200459, 2023.
- [26] J. Liu, Y. Zhang, X. Zhao, and Z. He, "Fr-lio: Fast and robust lidar-inertial odometry by tightly-coupled iterated kalman smoother and rocentric voxels," *arXiv preprint arXiv:2302.04031*, 2023.
- [27] A. Gelb, *Applied Optimal Estimation*. MIT Press, 1974.
- [28] J. Sola, "Quaternion kinematics for the error-state kf," *Laboratoire d'Analyse et d'Architecture des Systemes-Centre national de la recherche scientifique (LAAS-CNRS), Toulouse, France, Tech. Rep.*, p. 35, 2012.
- [29] C. Hertzberg, R. Wagner, U. Frese, and L. Schröder, "Integrating generic sensor fusion algorithms with sound state representations through encapsulation of manifolds," *Information Fusion*, vol. 14, no. 1, pp. 57–77, 2013.
- [30] J. Li, W. Wu, B. Yang, X. Zou, Y. Yang, X. Zhao, and Z. Dong, "Whu-helmet: a helmet-based multisensor slam dataset for the evaluation of real-time 3-d mapping in large-scale gnss-denied environments," *IEEE Transactions on Geoscience and Remote Sensing*, vol. 61, pp. 1–16, 2023.
- [31] Y. Liu, Y. Fu, M. Qin, Y. Xu, B. Xu, F. Chen, B. Goossens, P. Z. Sun, H. Yu, C. Liu *et al.*, "Botanicgarden: A high-quality dataset for robot navigation in unstructured natural environments," *IEEE Robotics and Automation Letters*, 2024.